A Novel Monolithic HEMT LNA Integrating HBT-Tunable Active-Feedback Linearization by Selective MBE

Kevin W. Kobayashi, *Member, IEEE*, Dwight C. Streit, *Senior Member, IEEE*, Aaron K. Oki, *Member, IEEE*, Donald K. Umemoto, *Member, IEEE*, and Thomas R. Block

***Abstract*— For the first time, a novel heterojunction bipolar transistor (HBT) active-feedback circuit is employed with a high electron mobility transistor (HEMT) low noise amplifier (LNA) which improves the linearity or third-order intercept point (IP3) and gain-bandwidth performance without significantly impacting noise figure. The HEMT and HBT circuits are monolithically integrated using selective molecular beam epitaxy (MBE). The use of HBT active feedback provides several advantages over field-effect transistor (FET) active feedback such as smaller size, lower dc power consumption, active self-bias, and direct-coupled performance. Applied to a 1–11 GHz HEMT LNA design, the HBT active feedback has resulted in a 50% improvement in gain-bandwidth performance and a 4–10 dB improvement in IP3 without degrading noise figure compared to an equivalent resistive-feedback design. In addition, the HBT active feedback consumes only 15% additional dc power and has provided as much as a 20-dB reduction in third-order (two-tone) intermodulation products (IM3's) over a narrow band. This HBT active-feedback linearization technique is a compact, cost-effective means of improving the linearity of HEMT-based LNA/receiver monolithic microwave/millimeter wave integrated circuits (MMIC's) for use in wireless multicarrier communications systems requiring a wide dynamic range.**

I. Introduction

In many commercial wireless communication systems where multicarrier reception is involved, a low noise amplifier (LNA) with high linearity performance is required. High electron mobility transistors (HEMT's) provide superior noise-figure performance compared to other technologies, however, they fall short of providing the best linearity performance. Fabrication techniques for improving the linearity or IP3 of field-effect transistor (FET) devices have been developed and have resulted in monolithic microwave/millimeter wave integrated circuits (MMIC's) with excellent IP3 performance [1]–[3]. However, compact low-cost designs, such as feedback amplifiers often used at lower frequencies, can provide only marginal improvement in linearity performance since the feedback will tend to dominate the circuit performance.

Several circuit techniques using concepts such as feedforward linearization and predistortion are popular circuit means for improving amplifier linearity performance [4]–[7]. However, these techniques involve complex methods or systems requiring precise control of phase, and amplitude characteristics are usually limited to narrow band applications and may require additional hardware that is not economically feasible to employ on an MMIC.

Other MMIC linearization techniques employing active and passive FET feedback have been developed to improve amplifier IMD performance as well as provide gain control function [8]–[10]. However, in these applications, FET feedback is used to improve the IMD performance under large-signal compressed conditions, but this feedback degrades amplifier noise-figure performance. Moreover, the FET feedback implementations consume substantial dc power and require dc-blocking capacitors which limit the effectiveness of the active feedback in suppressing the baseband intermodulation (IM) beat tones and can significantly increase the circuit area. On the other hand, employing heterojunction bipolar transistor (HBT) bipolar active feedback can result in smaller size and less dc power while providing active self-bias and direct-coupled performance which allow more effective suppression of the baseband IM beat tones. Therefore it is highly desirable to implement the active feedback using high-speed bipolar devices such as HBT's.

Using a recently developed HEMT HBT selective molecular beam epitaxy (MBE) multifunctional IC-integration technology [11], a tunable HBT active-feedback circuit is integrated with a HEMT LNA which improves both the small-signal gain-bandwidth and linearity (IP3) performance without sacrificing the noise-figure performance, or significantly increasing chip size and dc power consumption. This work underscores a prime example of the size and performance benefits which can be obtained in an MMIC using HEMT HBT multifunction selective MBE IC technology.

II. HEMT HBT Selective MBE IC Technology

The HEMT HBT MMIC of this work was fabricated using selective MBE IC technology. This HEMT HBT technology has previously been reported and described in detail [11], [12]. The selective MBE techniques used here are based on silicon nitride definition and patterning of molecular beam epitaxial layers, and they are similar in concept to the techniques we have previously used to fabricate complementary npn-pnp HBT circuits [13]–[16]. The GaAs-AlGaAs HBT structure is grown first using our baseline process. This HBT MBE profile

Manuscript received April 1, 1996.

The authors are with TRW, Inc., Electronics Systems and Technology Division, Redondo Beach, CA 90278 USA.

Publisher Item Identifier S 0018-9480(96)08536-5.

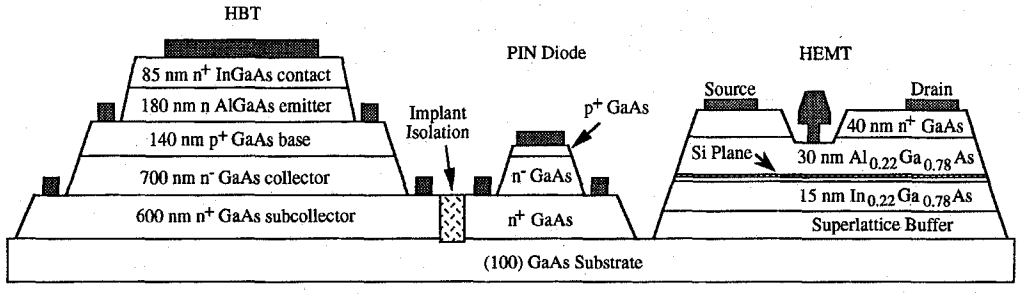

Fig. 1. Cross section of the HEMT HBT selective MBE IC technology.

is optimized for TRW's high-linearity applications and has shown excellent circuit reliability with a mean time to failure $>10^7$ h at a junction temperature of 125° based on three temperature life tests and operating under a maximum current density of $J_c \approx 27$ kA/cm^2 [17]. The HBT wafer is patterned with silicon nitride deposited by plasma-enhanced chemical vapor deposition. The silicon nitride and HBT layers are selectively etched to form HBT material islands. The patterned wafer is then cleaned and reintroduced into the MBE system for HEMT material growth. The pseudomorphic InGaAs-GaAs HEMT layer is grown using our normal HEMT growth procedures forming high-quality epitaxial material in areas where the HBT material has been removed. A merged HEMT HBT process technology was developed to allow a common process to be used for both the HEMT and HBT devices. The remainder of the process includes thin-film resistors, airbridges within islands and between HEMT and HBT islands, wafer thinning, and backside vias. Fig. 1 shows a cross section of the resulting HBT PIN HEMT integrated circuit technology.

This technology integrates 0.2-μm gate-length pseudomorphic InGaAs-GaAs HEMT's and 2-μm emitter-width self-aligned base-ohmic metal GaAs-AlGaAs HBT's. The HEMT and HBT devices produced by selective MBE and fabricated using a merged HEMT HBT process exhibit dc and microwave performance equivalent to devices fabricated using conventional MBE and our baseline single-technology processes [11], [12]. Using our baseline profiles with the selective MBE process, the 0.2-μm HEMT devices achieved $g_m = 600$ mS/mm, $f_T = 80$ GHz, and corresponding $f_{\max} = 150$ GHz. The 2-μm HBT devices achieved $\beta = 60$ at $J_c = 20$ kA/cm^2, $f_T = 22$ GHz, and $f_{\max} = 50$ GHz.

Using this process several HEMT HBT MMIC demonstrations have previously been reported which illustrate various combinations of monolithically integrated circuit functions such as HBT bias-regulated HEMT LNA [11], [18], HEMT switch with integrated HBT switch driver [19], and cascaded HEMT LNA with HBT output driver [20] MMIC's. These MMIC's demonstrate IC functions which would otherwise be integrated discretely in a hybrid, and thus, reduce the size, integration complexity, and cost of the integrated microwave assembly while offering the performance benefits of both HBT and HEMT device technologies. However, the linearized HEMT LNA MMIC of this work along with a previously reported common-gate (CG) HEMT actively matched HBT amplifier MMIC [21] provide additional performance benefits which arise from unique combinations of HEMT and HBT circuit techniques. It is the exploitation of these complimentary FET and bipolar circuit techniques that results in compounded benefits. This makes the HEMT HBT integration technology even more attractive and is the underlying theme embodied in this work.

III. HEMT LNA WITH HBT ACTIVE-FEEDBACK DESIGN

Active-device techniques are useful for achieving enhanced circuit performance without significantly impacting size or cost. HBT active-feedback techniques have previously been developed to economically implement regenerative feedback in amplifiers [22], [23]. Normally implemented as a spiral inductor in the parallel feedback loop in microwave circuits, regenerative feedback is used to extend the upper band gain response. In HBT bipolar technology, active feedback can be implemented with small 2×10-μm^2 emitter-area transistors instead of large spiral inductors which are 10–20 times larger. A previously reported HBT active-feedback technique has been shown to increase the bandwidth of HBT amplifiers by 50% [22]. In recent literature, FET active feedback [9] has been shown to improve the IMD performance of amplifiers due to its unilateral feedback characteristics. However, it consumes more circuit real estate and dc power compared to an equivalent HBT bipolar implementation. Thus, by employing HBT's with HEMT's on the same substrate, HBT active feedback can be integrated with HEMT's to improve their linearity performance with minimal impact on chip size and dc power consumption. In this manner, the potential benefits which each device technology offers can be fully exploited.

Using our HEMT HBT selective MBE integration technology, a novel HBT active-feedback network [22], [23] was integrated with a low-noise HEMT device to create a high-linearity LNA. Fig. 2 gives a schematic of the HEMT LNA which incorporates HBT-tunable active feedback. Active feedback constructed using bipolar or HBT transistors is preferred over FET or HEMT transistor implementations because they offer lower dc current and power consumption, are easier to self-bias, require no dc-blocking capacitors, and can be implemented in a smaller area. The low noise-figure performance of the amplifier is provided by a 0.2×200-μm^2 gate-area HEMT device M1, which is nominally biased at $I_{ds} = 20$ mA and $V_{ds} = 2$ V. A load resistor, R_{load}, provides an ac load at the drain of $M1$ as well as a means of setting up the quiescent dc bias of $M1$ through supply voltage V_{dd}. The supply voltage is 5 V and consumes between 20–25 mA depending on the active-feedback tuning

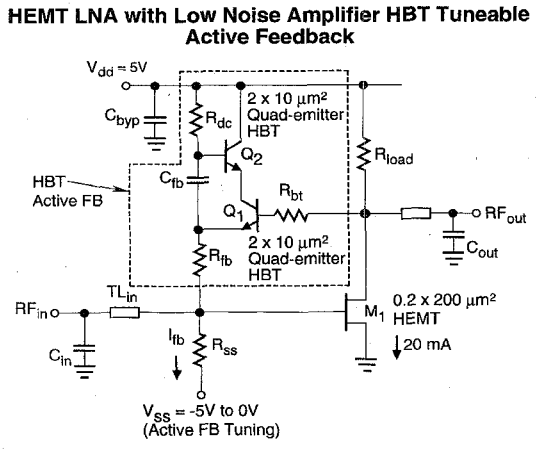

Fig. 2. Schematic of the HEMT LNA which integrates HBT-tunable active feedback.

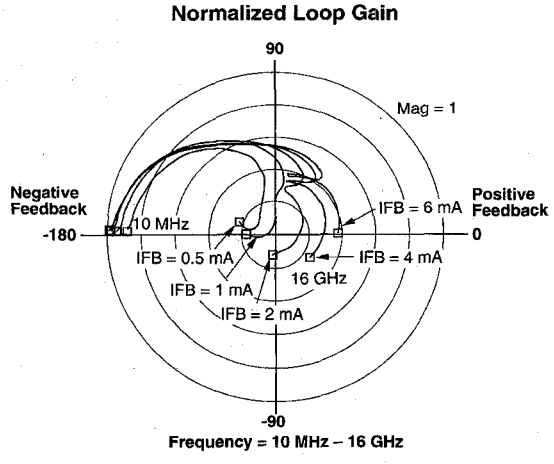

Fig. 3. Simulated (10 MHz–16 GHz) normalized loop gain and phase response of the amplifier for various feedback bias current I_{fb} = 0.5, 1, 2, 4, 6 mA.

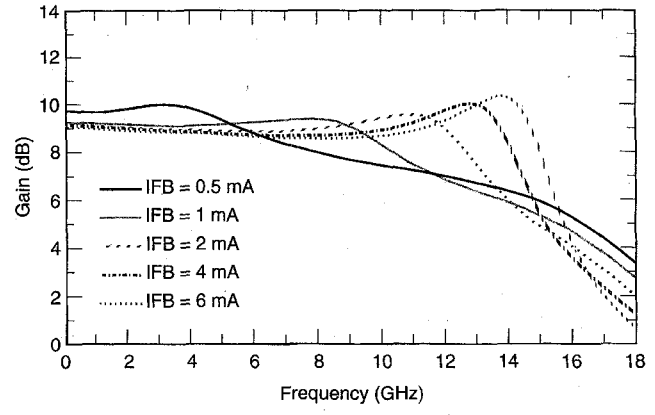

Fig. 4. Simulated amplifier gain response for various feedback bias current I_{fb} = 0.5, 1, 2, 4, 6 mA.

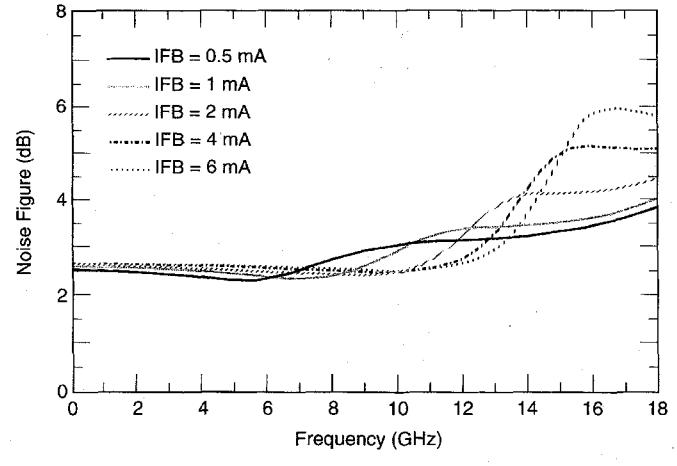

Fig. 5. Simulated amplifier noise-figure response for various feedback bias current I_{fb} = 0.5, 1, 2, 4, 6 mA.

bias condition. The tunable HBT active-feedback network is comprised of cascode connected HBT transistors Q_1 and Q_2, regenerative-feedback tuning resistor R_{bt}, dc bias resistor $R_{\rm dc}$, and ac-feedback capacitor C_{fb}. The HBT devices are 2×10-μm^2 four-finger (quad) emitter devices biased at an I_{cc} (I_{fb}) of between 0.5–4 mA. In a previous demonstration, this cascode HBT active-feedback topology was shown to be more effective in achieving regenerative feedback than a single HBT transistor active-feedback employment [23]. However, its electronic tunability and linearity enhancement has not been reported until now. The active HBT feedback is in series with a feedback resistor R_{fb} which provides a nominal amount of resistive feedback. Resistor R_{bt} can be set to achieve regenerative feedback from the HBT active-feedback network as has been previously demonstrated [22].

The bias current of the active-feedback circuit I_{fb} can be adjusted by varying the supply voltage V_{ss} from -1 V to -5 V. This range in tuning voltage corresponds to an adjustment of active-feedback current I_{fb} from 0.5–3.6 mA. By adjusting V_{ss}, various degrees of positive feedback can be induced by the resultant change in phase and amplitude characteristics of the active-feedback network. This is illustrated in Fig. 3 which gives the broadband (10 MHz–16 GHz) normalized loop gain and phase response of the amplifier for various feedback bias currents I_{fb}. This figure illustrates relative changes in loop gain and phase response and shows a total loop phase of almost 360° (0°) at 16 GHz for higher I_{fb} currents, demonstrating the onset of positive feedback through electronic tuning. Figs. 4 and 5 give the corresponding simulated amplifier gain and noise-figure response over active-feedback bias tuning. Fig. 4 shows a typical gain of 9 dB at low frequencies and illustrates gain peaking at the upper band edge for higher I_{fb}. A gain-bandwidth enhancement of 28% is predicted from this figure with as much as 1.5 dB of controlled gain peaking. Under these conditions, the simulated response was unconditionally stable. Fig. 5 shows the corresponding noise-figure dependence on active-feedback bias tuning. In the practical band of interest, usually below the gain-peaking frequency, the noise figure is 2.5 dB and seems to be insensitive to active-feedback bias. At the upper band edge under the conditions where regenerative feedback is pronounced, the noise figure degrades corresponding to noise regeneration. However, it is outside the frequency band of interest.

Fig. 6 shows a microphotograph of the fabricated HEMT HBT LNA MMIC. The HEMT LNA and HBT active feedback

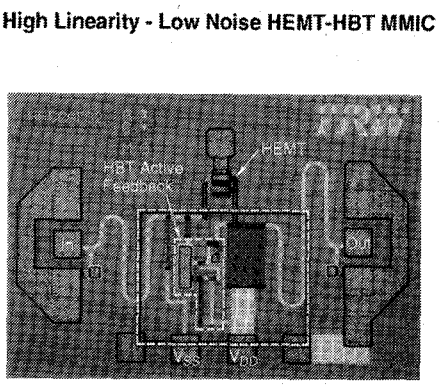

Fig. 6. Microphotograph of the fabricated high-linearity low-noise HEMT HBT MMIC.

consume as little as 300 μm $\times$ 300 μm without bond pads and transmission lines. Note the compact size of the HBT active-feedback network which requires no dc-blocking capacitors, and it is much smaller than a spiral inductor implementation. Moreover, the HBT active feedback offers direct-coupled performance as opposed to an FET implementation. This broadband (down to dc) feedback performance is believed to reduce intermodulation distortion (IMD) by allowing negative feedback at baseband frequencies which suppresses the IM beat tones that are generated. In conventional hybrid designs, these baseband beat products are normally bypassed to ground at the input and output of the amplifier using large off-chip bypass capacitors. The employment of HBT direct-coupled active feedback provides a completely monolithic solution to this problem.

IV. Measured Performance

Fig. 7 gives the measured gain response for different HBT active-feedback bias currents I_{fb} and also a typical input and output return-loss response for the maximally flat-gain feedback bias condition (I_{fb} = 2 mA). The nominal gain is 9 dB with 3-dB bandwidths greater than 11 GHz. This is consistent with the simulated performance. As the voltage supply V_{ss} is decreased from -1 V to -5 V, the feedback bias current increases. This changes the amplitude and phase characteristics through the HBT active-feedback network such that more positive feedback is employed at the higher frequencies as already discussed. Fig. 7 illustrates the resultant gain peaking which was measured over various feedback bias currents. At one extreme (V_{ss} = -5 V and I_{fb} = 3.6 mA) you get excessive gain peaking; at the other extreme (V_{ss} = -1 V and I_{fb} = 0.5 mA), the gain has a pronounced rolloff. At V_{ss} = -3 V and a feedback current of 2 mA, the gain has a maximally flat response up to 11 GHz with about 0.5-dB gain peaking at 13 GHz. The corresponding input and output return losses at this tuning voltage are greater than 10 dB across the band. Fig. 8 gives a plot of the measured and simulated 3-dB bandwidth versus active-feedback current I_{fb}. In general, the measured tuning bandwidth characteristics show that less current is actually required to achieve positive feedback than what was simulated. However, it should be noted that the 3-dB bandwidth (BW) is

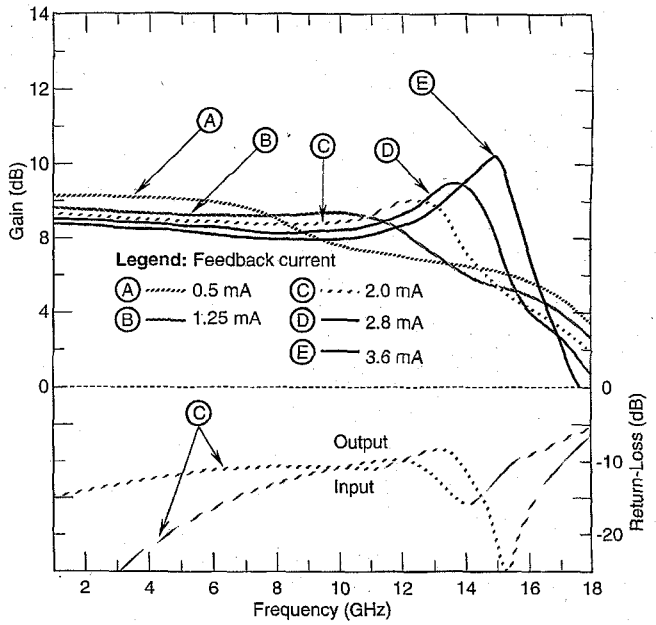

Fig. 7. Measured gain response for different HBT active-feedback bias currents I_{fb} and typical input and output return losses at the maximally flat-gain bias (I_{fb} = 2 mA).

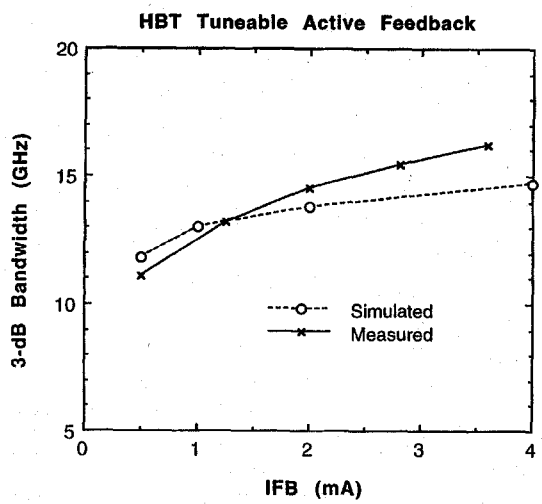

Fig. 8. Simulated and measured amplifier 3-dB bandwidth versus active-feedback current I_{fb}.

sensitive to device performance and that the general concept of tunable-regenerative active feedback was demonstrated and is consistent with the simulated performance. This figure also illustrates that the measured 3-dB BW was improved from 11 GHz to greater than 16 GHz by adjusting the active-feedback bias. The net result is a 50% BW enhancement using this technique.

A radical improvement in measured IP3 was also achieved by bias-tuning the HBT active feedback. Fig. 9 shows the measured two-tone IP3 response as a function of active-feedback bias (V_{ss} and I_{fb}). Also shown for reference is the IP3 response of a resistive-feedback HEMT LNA design (bold line) without the HBT active feedback which is nominally 20 dBm. This plot shows that as the HBT active-feedback bias is increased and the loop gain and phase are changed

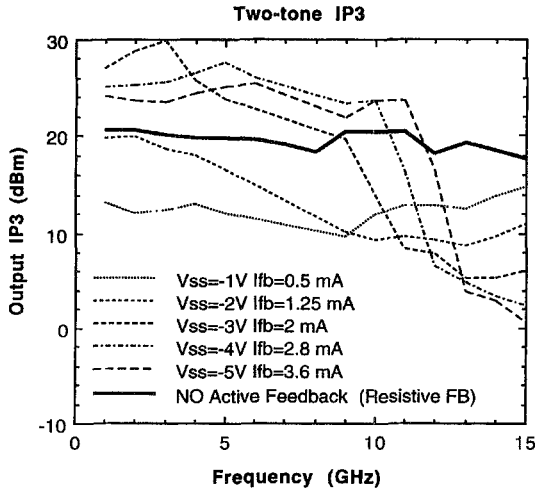

Fig. 9. Measured two-tone IP3 over frequency for various active-feedback bias conditions (V_{ss} and I_{fb}). Also shown is the 20-dBm IP3 reference (bold line) of a conventional-resistive HEMT LNA design without HBT active feedback.

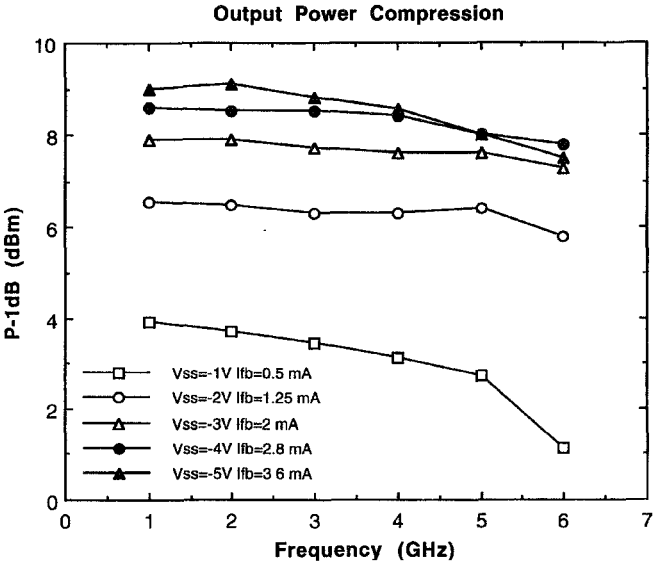

Fig. 10. Measured 1-dB compression point over a 1–6 GHz frequency band for the various active-feedback bias conditions.

to induce positive feedback at the upper band edge, the IP3 begins to increase at the lower frequencies. As the bias is further increased, the IP3 performance begins to significantly exceed the resistive-feedback HEMT LNA design at the lower frequencies below 8 GHz. For example, at $V_{ss} = -3$ V ($I_{fb} = 2$ mA), the IP3 is as great as 27–30 dBm which is an improvement of 7–10 dB over the conventional resistive-feedback HEMT LNA for frequencies from 1–3 GHz. As the bias is further increased, the IP3 performance begins to improve at the higher band edge. At a $V_{ss} = -5$ V ($I_{fb} = 3.6$ mA), the IP3 is 24 dBm across the 1–11 GHz band which is a 4-dB improvement over the resistive-feedback HEMT (no active feedback) amplifier. This improvement in IP3 and associated gain-bandwidth performance is at the expense of an additional 3 mA of current or only a 15% increase in dc power.

Fig. 10 gives the 1-dB compression performance over a 1–6 GHz frequency band for the different active-feedback bias points. These curves illustrate that the $P_{-1\text{dB}}$ is dependent on active-feedback current. At a low I_{fb} bias of 0.5 mA, the HBT active feedback is limiting the $P_{-1\text{dB}}$ of the amplifier, and the effects of the active feedback on bandwidth performance are observed. At higher bias currents, the $P_{-1\text{dB}}$ of the amplifier starts to saturate at ≈ 8 dBm and is flat across the band.

Fig. 11 gives the output IP3 and $P_{-1\text{dB}}$ of the HEMT LNA over the HBT active-feedback current bias at 1, 3, and 5 GHz. The 20-dBm IP3 level of the HEMT resistive-feedback LNA with "no HBT active feedback" is given as a reference. This figure shows that the $P_{-1\text{dB}}$ point increases from 3 dBm to 9 dBm as I_{fb} (feedback current) is increased. At 1, 3, and 5 GHz the $P_{-1\text{dB}}$ response is nearly identical. The IP3 initially increases with I_{fb}, reaches a maximum IP3 which is 6–10 dB greater than the 20-dBm IP3 of the conventional HEMT LNA, and then slightly decreases at higher I_{fb}. For a given frequency of 3 GHz, a 10-dB improvement is achieved at $I_{fb} = 2$ mA relative to the conventional resistive-feedback HEMT LNA. At higher frequencies, more active-feedback bias is required in order to enhance the IP3. For example, at 5 GHz an optimum IP3 of 27 dBm is achieved at slightly higher $I_{fb} = 2.8$ mA. The enhanced linearity of the HEMT LNA due to the HBT active feedback is frequency dependent as illustrated in Figs. 9 and 11. This suggests that the active-feedback phase which is frequency dependent is compensating for the less than ideal 180 out-of-phase required for negative feedback at the fundamental third-order (two-tone) intermodulation product (IM3) and baseband IM3 beat frequencies. Another contributing factor impacting the IM3 performance is the feedback of the 2nd harmonic. It has been demonstrated that with the proper phase, the 2nd harmonic can be fed back to the input of the amplifier to generate IM3 product terms which are opposite in sign to the original IM3 products generated from the nonlinearities of the amplifier, thus, resulting in a cancellation of the IM3 products generated at the output [24]. To ascertain the weight of each mechanism which reduces the IM3 distortion requires the development of large-signal HEMT and HBT models which can accurately model these small-signal nonlinearities. This is left for future work.

Another figure of merit used as a measure of linearity performance is the delta between the IP3 and $P_{-1\text{dB}}$ compression points (also illustrated in Fig. 11). In a conventional HEMT amplifier, the IP3 is about 10 dB higher than the $P_{-1\text{dB}}$ compression point as illustrated by the IP3 and $P_{-1\text{dB}}$ performance of the conventional design. A delta which is significantly greater than 10 dB would indicate an improvement in linearity performance. At the optimum I_{fb} bias for each frequency, the IP3-$P_{1\text{dB}}$ delta is between 17–20 dB which corresponds to a 7–10 dB improvement in this measure of linearity.

However, the use of both IP3 and the delta between the IP3 and $P_{-1\text{dB}}$ are only figures of merit and may not accurately portray the linearity characteristics of the amplifier circuit. The linear properties of the amplifier can be examined in greater detail in Figs. 12 and 13 which plot the fundamental (single-tone) output power (P_{out}) and IM3 versus input power (P_{in}) at 1 and 3 GHz. These plots compare the conventional

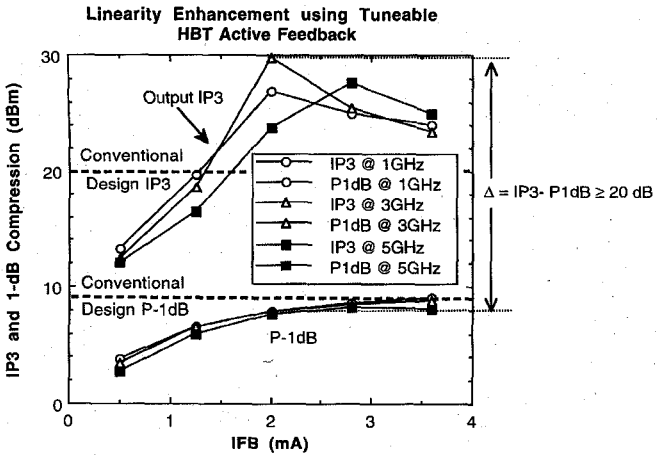

Fig. 11. Output IP3 and $P_{-1\text{dB}}$ for various active-feedback bias conditions at 1, 3, and 5 GHz.

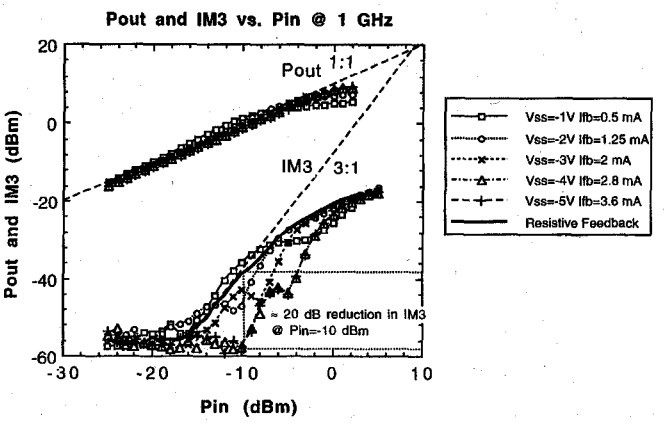

Fig. 12. P_{out} and IM3 vs. P_{in} at 1 GHz. Also shown for reference is the resistive-feedback HEMT LNA response.

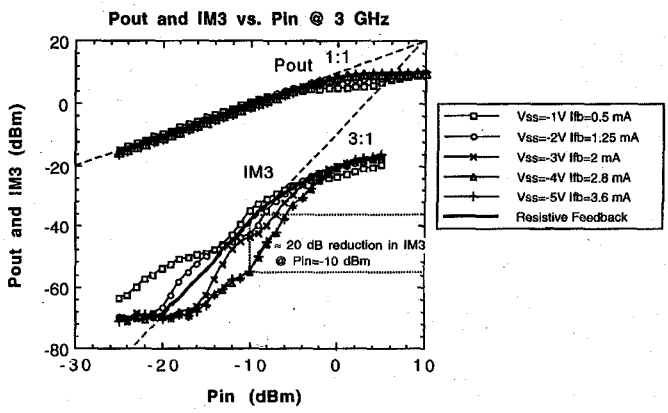

Fig. 13. P_{out} and IM3 vs. P_{in} at 3 GHz. Also shown for reference is the resistive-feedback HEMT LNA response.

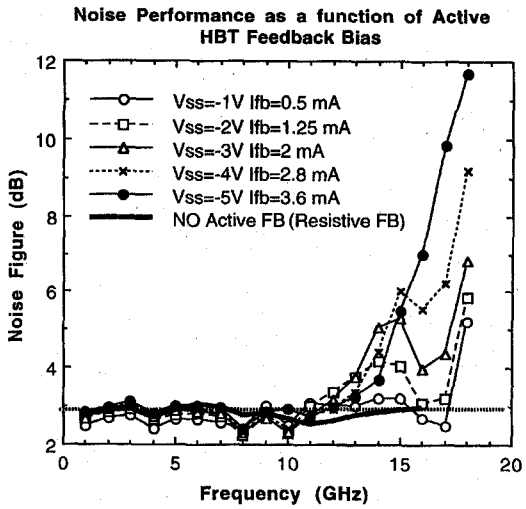

Fig. 14. Noise-figure response for the various active-feedback bias conditions. Also shown for reference is the noise-figure response of the resistive-feedback HEMT LNA design.

resistive-feedback HEMT LNA to the HBT-tunable active-feedback HEMT LNA. At both 1 and 3 GHz, as the HBT active-feedback current I_{fb} is increased, the IM3's become suppressed below the conventional resistive-feedback design in the input power range where the amplifier is operating linearly (−20–0 dBm). As much as 18–20 dB improvement in IM3 suppression can be seen at an input power of −10 dBm. At low I_{fb} bias, the IM3 performance is slightly worse than the pure resistive-feedback case due to nonlinearities generated by the HBT active-feedback devices. Above an I_{fb} of 1.25 mA, the IM3 product level drops well below the conventional resistive-feedback case where an IM3:Pin slope of 3:1 is recorded. This indicates that the active feedback is effectively canceling out the IM3 products, leaving higher order residual products. Thus, these detailed IM3 vs. input power measurements indicate a large improvement in linearity performance due to the HBT active feedback.

The HEMT LNA noise-figure performance was also found to be insensitive to the use of the HBT active feedback. Fig. 14 shows the noise-figure response as a function of the active-feedback tuning bias. Also shown for reference is the noise-figure response of the conventional resistive-feedback HEMT LNA with "no HBT active feedback." The nominal noise figure of the amplifier is 3 dB and essentially flat from 1–11 GHz. This is slightly higher than the nominal noise figure of 2.5 dB predicted from the simulations. The noise-figure performance is not sensitive to the active-feedback bias and is comparable to the resistive-feedback HEMT LNA design in this frequency band where the gain was found to be maximally flat. Above 11 GHz where gain peaking is induced at higher I_{fb} feedback bias, the noise figure also begins to abruptly degrade. This illustrates the effect of positive feedback which regenerates the noise amplitude as well as the desired signal, resulting in gain peaking and noise-figure degradation. This was also predicted from simulations. However, this noise-figure degradation occurs at frequencies beyond the practical 1–11 GHz bandwidth of the amplifier where a desired flat-gain response is achieved.

V. Conclusion

A novel high-linearity low-noise HEMT LNA which integrates HBT-tunable active feedback has been presented. The HEMT HBT MMIC was fabricated using selective MBE technology. The active HBT feedback circuit enhances the

gain-bandwidth and linearity performance without compromising the noise figure of the amplifier. The active HBT feedback can be electronically tuned to achieved a 50% improvement in gain-bandwidth and a corresponding 7–10 dB improvement in IP3 (linearity) performance while consuming only 2–3.6 mA of additional current through the active-feedback network. The authors believe that this work demonstrates the potential size and performance advantages of the HEMT HBT selective MBE technology which can ultimately provide benefits for high-volume commercial applications.

ACKNOWLEDGMENT

The authors would like to thank T. Naeole for HBT fabrication, M. Iiyama for layout, G. Fisk for RF test support, and special thanks to Dr. P. Liu and the EBL group for HEMT gate processing.

REFERENCES

[1] S. L. G. Chu, J. Huang, W. Struble, G. Jackson, N. Pan, M. J. Schindler, and Y. Tajima, "A highly linear MESFET," in *1991 IEEE MTT Symp. Dig.*, Boston, MA.

[2] W. Struble, S. L. G. Chu, M. J. Schindler, Y. Tajima, and J. Huang, "Modeling intermodulation distortion in GaAs MESFET's using pulsed *I-V* characteristics," in *1991 IEEE GaAs IC Symp. Dig.*, Monterey, CA, pp. 179–182.

[3] S. L. G. Chu, J. C. Huang, A. Bertrand, M. J. Schindler, W. Struble, R. Binder, and W. Hoke, "High linearity monolithic broadband pseudomorphic spike-doped MESFET amplifiers," in *1992 IEEE GaAs IC Symp. Dig.*, Miami, FL, pp. 211–214.

[4] H. Seidel, "A feedforward experiment applied to an L-4 carrier system amplifier," *IEEE Trans. on Commun. Technol.*, vol. COM-19, no. 3, pp. 320–325, June 1971.

[5] A. Katz, S. Moochalla, and J. Klatskin, "Passive FET MMIC linearizers for C, X and Ku-band satellite applications," in *1993 IEEE MMWMC Symp. Dig.*, Atlanta, GA, pp. 155–158.

[6] A. Katz, R. Sudarsanam, and D. Aubert, "A reflective diode linearizer for spacecraft applications," in *1985 IEEE MTT Symp. Dig.*, St. Louis, MN, pp. 661–664.

[7] R. Inada, H. Ogawa, S. Kitazume, and P. Desantis, "A compact 4-GHz linearizer for space use," *IEEE Trans. Microwave Theory Tech.*, vol. MTT-34, no. 12, Dec., 1986, pp. 1327–1986.

[8] M. Muraguchi and M. Aikawa, "A linear limiter: A 11 GHz monolithic low distortion variable gain amplifier," in *1991 IEEE MTT Symp. Dig.*, Boston, MA, pp. 525–528.

[9] K. Nishikawa and T. Tokumitsu, "An MMIC low-distortion variable-gain amplifier using active feedback," in *1995 IEEE MTT Symp. Dig.*, Orlando, FL, pp. 1619–1622.

[10] J. C. Pedro and J. Perez, "An MMIC linearized amplifier using active feedback," in *1993 IEEE MMWMC Symp. Dig.*, Atlanta, GA, pp. 113–116.

[11] D. C. Streit, D. K. Umemoto, K. W. Kobayashi, and A. K. Oki, "Monolithic HEMT-HBT integration by selective MBE," *IEEE Trans. Electron Devices*, vol. 42, no. 4, pp. 618–623, Apr. 1995.

[12] D. K. Umemoto, D. C. Streit, K. W. Kobayashi, and A. K. Oki, "35 GHz HEMT amplifiers fabricated using integrated HEMT-HBT material grown by selective MBE," in *IEEE Microwave Guided Wave Lett.*, vol. 4, no. 11, Nov. 1994.

[13] D. C. Streit, D. K. Umemoto, J. R. Velebir, K. W. Kobayashi, and A. K. Oki, "Selective molecular beam epitaxy for integrated npn/pnp heterojunction bipolar transistors," *J. Vac. Sci. Technol. B, Microelectron Process Phenom.*, vol. B-10, pp. 1020–1022, 1992.

[14] D. K. Umemoto, J. R. Velebir, K. W. Kobayashi, A. K. Oki, and D. C. Streit, "Integrated npn/pnp GaAs/AlGaAs HBT's grown by selective MBE," *Electron. Lett.*, vol. 27, pp. 1517–1518, 1991.

[15] K. W. Kobayashi, D. K. Umemoto, J. R. Velebir, A. K. Oki, and D. C. Streit, "Complementary HBT push-pull amplifier by selective MBE," *IEEE Microwave Guided Wave Lett.*, vol. 2, pp. 149–150, 1992.

[16] ——, "Integrated complementary HBT microwave push-pull and Darlington amplifiers with p-n-p active loads," *IEEE J. Solid-State Circuits*, vol. 28, pp. 1011–1017, 1993.

[17] F. M. Yamada, A. K. Oki, D. C. Streit, Y. Saito, A. R. Coulson, W. C. Atwood, and E. A. Rezek, "Reliability of a high performance monolithic IC fabricated using a production GaAs/AlGaAs HBT process," in *1994 IEEE GaAs IC Symp. Dig.*, Philadelphia, PA, pp. 271–274.

[18] K. W. Kobayashi, D. K. Umemoto, T. R. Block, A. K. Oki, and D. C. Streit, "A wideband HEMT cascode low-noise amplifier with HBT bias regulation," *IEEE Microwave Guided Wave Lett.*, vol. 5, no. 12, pp. 457–459, Dec. 1995.

[19] K. W. Kobayashi, A. K. Oki, L. B. Sjogren, D. K. Umemoto, T. R. Block, and D. C. Streit, "A monolithic HEMT passive switch with integrated HBT standard logic compatible driver for phased array applications," *IEEE Microwave Guided Wave Lett*, to be published.

[20] K. W. Kobayashi, D. K. Umemoto, T. R. Block, A. K. Oki, and D. C. Streit, "A novel monolithic LNA integrating a common-source HEMT with an HBT darlington amplifier," *IEEE Microwave Guided Wave Lett.*, vol. 5, no. 12, pp. 442–444, Dec. 1995.

[21] ——, "A monolithic HEMT-HBT direct-coupled amplifier with active input matching," *IEEE Microwave Guided Wave Lett.*, vol. 6, no. 1, pp. 55–57, Jan. 1996.

[22] K. W. Kobayashi, L. T. Tran, J. R. Velebir, A. K. Oki, and D. C. Streit, "A novel active feedback design using InAlAs/InGaAs heterojunction bipolar transistors," *IEEE Microwave Guided Wave Lett.*, vol. 4, no. 5, pp. 146–148, May 1994.

[23] K. W. Kobayashi, D. C. Streit, D. K. Umemoto, and A. K. Oki, "A novel monolithic HBT-p-i-n-HBT integrated circuit with HBT feedback and p-i-n diode variable gain control," *IEEE Trans. Microwave Theory Tech.*, vol. 43, no. 5, pp. 1004–1009, May 1995.

[24] M. R. Moazzam and C. S. Aitchison, "A low third order intermodulation amplifier with harmonic feedback circuitry," in *1996 IEEE Microwave Theory Techniques Symp. Dig.*, San Francisco, CA, June 1996, pp. 827–830.

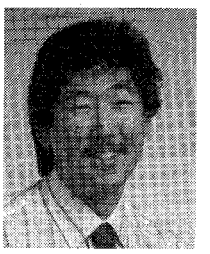

Kevin W. Kobayashi (M'93) was born in San Diego, CA, in 1963. He received the B.S.E.E. degree from the University of California at San Diego in 1986 and the M.S.E.E. degree from the University of Southern California in 1991.

Since 1986 he has been working at TRW's Advanced Microelectronics Laboratory, Redondo Beach, CA, where he has been involved in the development of HBT, HEMT, and MESFET technologies. He is currently a Staff Engineer focused on the design of HBT and HEMT MMIC's for insertion into TRW systems and a Principal Investigator of MMIC Linearization IR&D activity. He also provides technical design support and instruction for TRW's GaAs HBT commercial foundry service. For the past few years he has been heavily involved with the design and development of selective MBE MMIC's which integrate HEMT's, HBT's, PIN's, and high-performance Schottky diodes on the same III-V substrate for next-generation high-performance mixed-mode MMIC applications. He has written several papers on MMIC design and technology and has been issued several related patents.

Dwight C. Streit (S'81–M'86–SM'92) received the Ph.D. degree in electrical engineering from the University of California, Los Angeles, in 1986.

He is currently an Assistant Manager of the Microelectronics Product and Technology Development Department and Manager of the RF Products Center, HEMT Technology Section at TRW, Inc., Redondo Beach, CA. He is a Principal Investigator for several research and development projects related to III-V materials, monolithic HEMT HBT integrated circuits, and quantum-effect devices.

Aaron K. Oki (M'85) was born in Honolulu, HI. He received the B.S. degree in electrical engineering in 1983 from the University of Hawaii at Manoa and the M.S. degree in electrical engineering and computer science in 1985 from the University of California at Berkeley.

Since joining TRW, Inc., Redondo Beach, CA, as a Member of the technical staff in 1985, he has been working on production and advanced development of HBT technology. In 1990 he became the Principal Investigator for HBT IR&D and Section Head of the HBT products section.

Donald K. Umemoto (M'88) received the B.S. degrees in biology and electrical engineering and the M.S. degree in electrical engineering from the University of Hawaii at Manoa in 1979, 1986, and 1988, respectively.

He joined TRW, Inc., Redondo Beach, CA, in 1988 as a Member of the technical staff of the HBT Technology Section in the GaAs IC Department. He is currently the Section Head of the Photolithography/Wet Etch Section of TRW's GaAs Flexible Manufacturing Process Laboratory.

Thomas R. Block was born in St. Louis, MO, in 1962. He received the B.S. degree in electrical engineering and the M.S. and Ph.D. degrees in engineering from the University of Texas at Austin in 1984, 1986, and 1991, respectively.

In 1991 he joined TRW, Inc., Redondo Beach, CA, as a Senior Member of Technical Staff engaged in molecular beam epitaxy growth of compound semiconductors for both research and production. He is involved in the growth of GaAs-based HBT's, HEMT's, MESFET's, and InP-based HBT's and HEMT's. In 1995 he became the Manager of the Advanced Materials Section at TRW.